Harishanker Chaudhary, et. al. International Journal of Engineering Research and Applications
www.ijera.com
ISSN: 2248-9622, Vol. 13, Issue 7, July 2023, pp 172-199

RESEARCH ARTICLE OPEN ACCESS

Numerical Modelling Of Tunnel Induced Settlement Using Finite Element Analysis

Harishanker Chaudhary and Sandeep Potnis
MTech, MIT, World Peace University

ABSTRACT
Future demond for computing capacities the use of 3D Finite element analysis in underground design has become more common.3D calculations are time consuming, and the necessary numerical tool was not always be available. In engineering practice empirical methods and 2D Finite Element analysis are used for tunnel design. The development of stresses and deformations due to tunnelling, however, is a complex three-dimensional problem. Reliable approximations are need. In this thesis tunnel induced settlements and internal lining forces are investigated for a non-circular tunnel in clay-/siltstone. The tunnel is constructed according to the principles of the New Austrian Tunnelling Method. 3D FE-analyses are compared with frequently used empirical methods and 2D FE-analyses. To account for three-dimensional stress redistribution in 2D the stress reduction method is used. Different reference values, constitutive models and stiffness parameters are compared. The obtained values are mainly influenced by the used reference value, ground water conditions and drainage type. Furthermore, the initial stress state and the soil model are shown to have an impact on the load reduction factor.
Key words: Plaxis 2D, Lining forces, Constitutive models, New Austrian Tunnelling Method.

Date of Submission: 08-07-2023 Date of acceptance: 20-07-2023

I. INTRODUCTION

In underground tunnel design the stability of the ground, along with surface settlements, deformations of the cavity and the resulting forces on the lining are of main interest. The development of stresses and deformations is a complex three-dimensional problem. However, in engineering practice commonly simple empirical methods and 2D FE- analyses are used. To account for the effects of three-dimensional stress-redistribution in 2D calculations approximation methods must be used. In open face tunnelling no support is applied on the tunnel face. It includes shield tunnelling without a pressurized face support and conventional tunnelling. Conventional tunnelling is characterized by an altering excavation and support sequence using shotcrete, anchors and steel arches as support means. Conventional tunnelling is often referred to as sprayed concrete method or New Austrian Tunnelling Method (NATM). The support can be adjusted to current ground conditions. Therefore, its use is very flexible. Over the last years the use of conventional tunnelling techniques in hard soil/soft rock (HSSR) increased. It includes hard, over- consolidated clays and soft sedimentary rocks (claystone, siltstone, weak limestone, etc.) The ground response is between that of rock and soil. Due to lower stability and larger deformations for tunnelling in HSSR ground the demands on support means are high. A fast ring-closure of the sprayed concrete lining and short round length help reducing settlements. The most common approximation method for modelling conventional tunnelling in 2D FE analysis is the stress-reduction method. In this thesis numerical calculations for a non-circular tunnel constructed in hard soil/soft rock using NATM are carried out with the commercial Finite Element code “PLAXIS 2D” and “PLAXIS 3D”. The results of the 3D calculations are compared to the suggested approximation procedure in 2D, empirical methods and field data. The focus is on the prediction of surface settlements, deformations of the tunnel and internal forces of the lining. The purpose is to achieve a better understanding of the influencing factors for the determination of the stress-reduction factor β to account for three.

II. TECHNICAL ADVANTAGE

SOIL MODELS The stress-strain-strength behaviour of soil a set of constitutive equations is used. Soil behaviour can be modelled with different degrees of accuracy. The simplest material model is linear-elastic and isotropic with only 2 input parameters. However, to obtain realistic results stress- and strain-dependent material properties of soil must be considered. A reasonable number of input parameters, which are physically relevant and can be measured, must be chosen. In this thesis calculations with the Mohr-Coulomb, Hardening Soil and HS-small model in PLAXIS are carried out.

MOHR-COULOMB MODEL The Mohr-Coulomb model is a linear-elastic, perfectly plastic model. Perfectly plastic models have a fixed yield surface f, which separates admissible and inadmissible states in stress space. Within the yield surface soil behaviour is purely elastic. The stress-strain relation is a bi-linear curve.

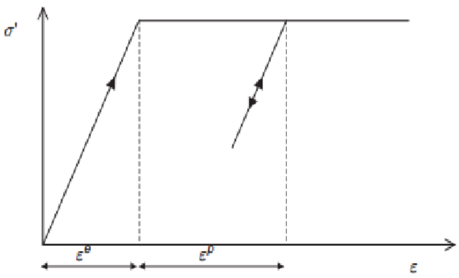

FIGURE 1: Stress-Strain Relation of a Linear-Elastic Perfectly Plastic Model [2]

No stress- and stress path dependency of stiffness is considered. The chosen soil stiffness E, which is known to be stress dependent, should be consistent with the developing stress level and stress path. Effective stress states near failure are described well by the model. The Mohr-Coulomb failure criterion is characterized by effective strength parameters, friction angle ϕ' and cohesion c'. In total five parameters are required: [2]

Young's modulus: E [kN/ m²]
Poisson ratio: ν [-]
Cohesion: c [kN/m²] –
Friction angle: ϕ [°] –
Dilatancy angle: ψ [°]

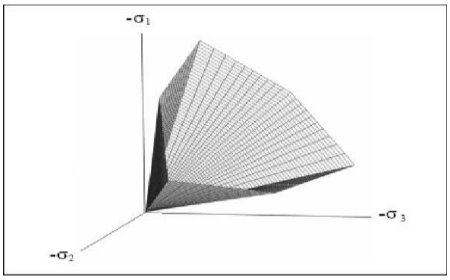

FIGURE 2: Mohr-Coulomb Yield Surface in Principal Stress Space for Cohesionless Soil

The Mohr-Coulomb model allows tensile stresses to develop in cohesive soils when shear stresses are small. However, experience shows that soil may fail in tension instead of in shear. In PLAXIS this can be considered by selecting the Tension cut-off. In this case no positive principal stresses are allowed. [2]. The Mohr-Coulomb model allows tensile stresses to develop in cohesive soils when shear stresses are small. However, experience shows that soil may fail in tension instead of in shear. In PLAXIS this can be considered by selecting the Tension cut-off. In this case no positive principal stresses are allowed.

HARDENING SOIL MODEL The Hardening Soil model is an isotropic hardening model. The yield surface is not fixed but expands with plastic straining. Two types of hardening can be distinguished. Shear hardening due to deviatoric loading is governed by the secant stiffness modulus E50 at 50% strength in triaxial testing. Compression hardening due to compression in oedometric and isotropic loading is governed by the oedometric stiffness Eoed. If no yield surface is active, soil behaviour is elastic. For un- and reloading the stress path is modelled as elastic using the higher stress-dependent stiffness Eur.

Input parameters for soil stiffness are:

Secant stiffness in standard drained triaxial test	$E^{50\ ref}$ [kN/m²]
Tangent stiffness for primary oedometer loading	E_{refoed} [kN/m²]
Power for stress-level dependency of stiffness	m [-]
Un-/reloading stiffness	Eu_{ur}^{ef} [kN/m²]
Poisson's ratio for un-/reloading	ν_{ur} [-]
Reference stress for stiffness's	p_{ref} [kN/m²]
Coefficient for lateral earth pressure at rest for normal consolidation	K [-]
Failure ratio (default value: 0.9)	Rf [-]

Stress dependency of stiffness is considered in the Hardening Soil model. The input stiffness parameters are defined for a reference stress level. E50 ref and E ref are related to the minor principal stress σ_3'. E_{oed}^{ref} is related to the vertical stress σ'1. The stress dependent stiffness is calculated by the relation $E = E^{ref}.(\sigma'1)\ p_{ref}$

One of the main advantages of the Hardening Soil model is the hyperbolic stress-strain curve for drained triaxial tests. The relationship between vertical strain ε1 and deviatoric stress q in primary triaxial loading is described by a hyperbolic curve as shown in Figure 3. The curve is representative for a fixed value of σ_3 [2]

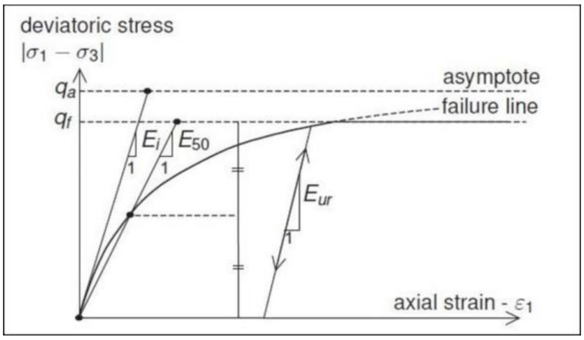

FIGURE 3: Hyperbolic Stress-Strain Relation in a Standard Drained Triaxial Test

$\varepsilon = {}^{q\,a\cdot q\,f\,o\,r\,q<q}$

1. $E_{50}q_{\;a-q}$
2. $q\,f = {}^{2}.{}^{\sin\emptyset}/_{1-\sin\emptyset}\,(c\,o\,t\,\emptyset - \sigma 3')$

Asymptotic value for shear strength
$q\,a = {}_{q\,f}{}^{R\,f}$
In Figure 4 the yield surfaces of the Hardening Soil model in two-dimensional p'-q plane is shown. Within the elastic region no yield surface is active and no plastic strains occur. In the blue marked region 1 the deviatoric yield surface is active.

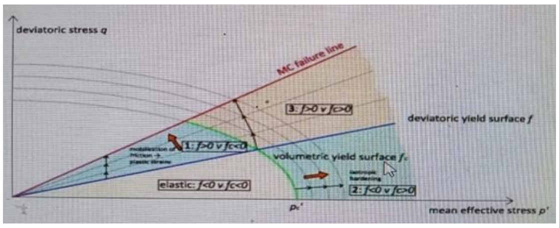

FIGURE 4: Yield Surfaces of the Hardening Soil Model In Two-Dimensional P'-Q Plane - Activation of Deviatoric and Volumetric Yield Surface

DEVIATORIC YIELD SURFACE The position of the deviatoric hardening surface f is related to mobilized friction and governed by E50. It represents lines of equal shear strains in triaxial tests with a constant hardening parameter γ^p. γ^p can be considered as the plastic shear strain related to the mobilized shear resistance. The shape depends on the power m and is a slighly curved line for values m < 1. The relationship between plastic shear strain γp and plastic volumetric strain v is given by the linear non-associated shear hardening flow rule [3]:

$$\varepsilon^{p} = s\,i\,n\,\varphi_{m}\gamma^{p}$$

The mobilized dilatancy angle φ_m is

$$s\,i\,n\,\varphi_{m} = {}^{\sigma\;1-\sigma\;1\,\sigma\;1-\sigma\;1-2./c\cdot c\,o\,t\,\varphi}$$

The equations (2.5), (2.6) and (2.7) are adapted from the stress-dilatancy theory by Rowe [4]. For small, mobilised friction angles plastic compaction is over predicted. Therefore, negative values of ψm are cut-off in PLAXIS. For ϕ = 0 the mobilised dilatancy angle is set equal to zero. At small stress ratios ϕm<ϕcv the material behavior is contractant, while at high stress ratios, when the mobilized friction angle exceeds the critical state friction angle, dilatancy occurs.

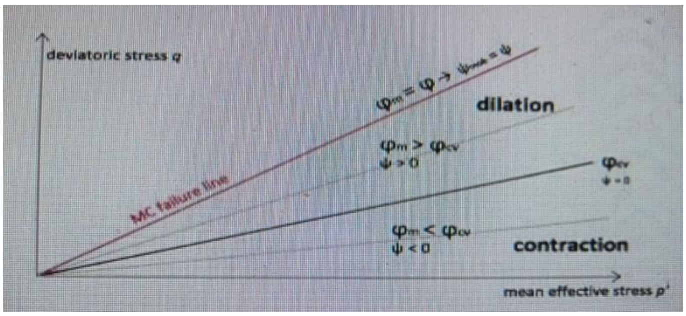

FIGURE 5: Shear Hardening Flow Rule - Mobilization of Friction

VOLUMETRIC YIELD SURFACE The volumetric yield surface fc is an ellipse in the q-p' plane. Its size is governed by the isotropic pre- consolidation pressure pc on the p-axis. pc is based on OCR (over-consolidation ratio) or POP (pre-overburden pressure). A more detailed description of the determination of initial stresses is given in chapter 3.4. On the q- axis the ellipse has a length of α*pc. α is an auxiliary parameter related to k^{nc}
The cap yield surface is defined by equation (2.8). [2]

$$f\,c = q^2 + p\,12 - p\,2\,/\alpha_2$$

With Volumetric stress

$$p^1 = \sigma\,1 + \sigma\,1 + \sigma\,1/3$$

Deviatoric stress

$$q\sim = \sigma\,1 + (\delta - 1).\sigma\,1 - \delta\,\sigma\,1$$

For volumetric yielding an associated flow rule is used. The plastic potential is defined as gc = fc.
The pre-consolidation stress $p_c$is related to volumetriccap strain $\varepsilon_v{}^{pc}$ by thehardening law:

$$\varepsilon_v{}^{pc} = \frac{\beta}{1-m}\left(\frac{p_p}{p^{ref}}\right)$$

2.3 HARDENING SOIL-SMALL MODEL

The Hardening Soil-small model is based on the Hardening Soil model and additionally considers strain dependency of stiffness at very small strains. The strain range at which soil behaviour can be considered truly elastic is very small. For the analysis of geotechnical structures small-strain stiffness and its non-linear strain-stiffness relationship should be taken into account. In addition to the Hardening Soil model two parameters are introduced: [2]

1. Initial or very small-strain shear modulus G0 at very sma-6ll strains, e.g. γ < 10
2. Shear strain level γ0,7 at which the secant shear modulus Gs is reduced to app. 70 % of G0

$G = G0\ / (1+0.385.\ \gamma\ )$

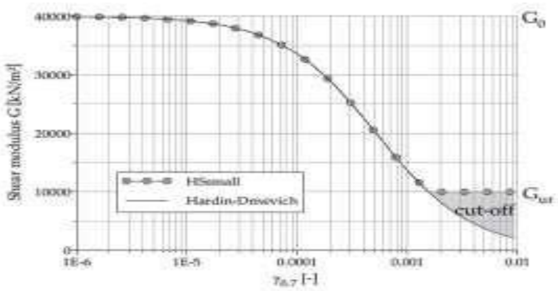

FIGURE 6 :Small-StrainStiffnessReductionCurveintheHardeningSoil-SmallModel

III. NUMERICAL MODEL

3.1. TUNNELGEOMETRY

The exploratory tunnel Mitterpichling is part of the investigation program for the Koralm tunnel. It is constructed as the top heading of the later to be built south tube of the final project using the New Austrian Tunnelling Method (NATM) [6]. The final tunnel cross section has a diameter of 10.0 m.

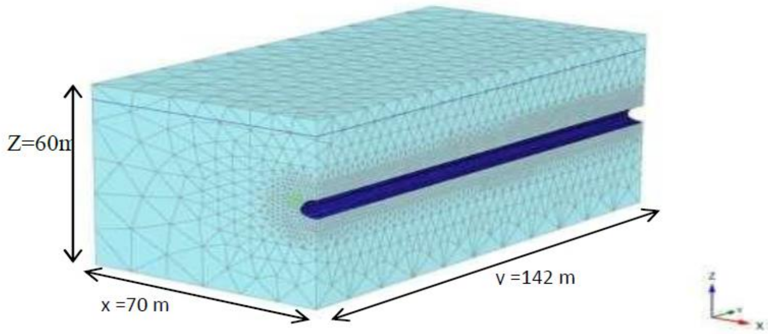

FIGURE 6: Numerical Model

indicating that the size of the model is sufficient. The excavation length for the calculation is 1.5 m. It is modelled as one slice. At the beginning and the end of the model 8 slices with 2.5 m (total 20.0 meters at each site) are modelled to bridge boundary conditions. For drained calculations this tunnel section is installed in one single phase ("wished-in-place"). In calculations considering groundwater conditions step-bystep excavation is modelled for the whole tunnel length. For the input of the tunnel cross section in PLAXIS 3D 2011 some adaptions have to be made. In the 2D version of the program circular arcs are modelled as curved lines. In the 3D version they are approximated by a linear polyline. The approximation is governed by input of the discretization angle. The discretization angle has to be chosen carefully because it influences the mesh quality around the tunnel.

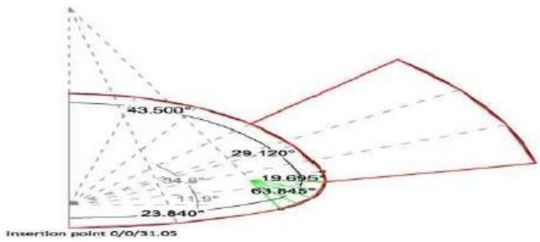

FIGURE 7: Cross-Section of the Tunnel

TABLE 1: Input Parameters Tunnel Cross-Section

	Secti on1	**Section**	**Section3**	**Secti on4**	**Secti on5**	**Secti onA**
Central Angle	23.84 0°	63.84 5°	19.685°	29.12 0°	43.50 0°	34.60 0°
Radius	9.9 m	1.4 m	1.4 m	5.0 m	5.0 m	9.0 m
Discretization	11.92 0°	15.96 1°	19.695°	14.56 0°	14.50 0°	11.53 0°

GROUND CONDITIONS For numerical calculations the tunnel section between station 1016 and 1187.5 of the exploratory tunnel Mitterpichling Ost is chosen. It can be considered as more or less homogeneous with dominant rock type silt- and claystone, slightly consolidated. The ground was previously loaded by a 25 m thick soil layer resulting in 500 kN/m² pre-overburden pressure. The groundwater table is about 5 m beneath the surface. The overburden in this section increases from 22.5 meters to 27.5 meters. Therefore, the considered average overburden is about 25 meters above the tunnel crown. The tunnel is supported by a 20 cm thick layer of shotcrete and anchors. No pipe roof is needed to secure the tunnel face. In the considered section tunnelling was carried out conventionally using blasting and excavators.

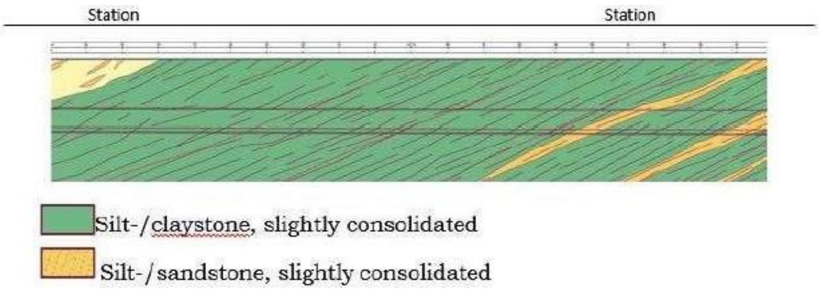

FIGURE 8: Geological Profile [8]

SOILPARAMETERS
No material parameters were available for the considered tunnel section. Hence, data from the adjoining construction lot Paierdorf for the same geological unit are adapted.

TABLE2: Material Parameters Gathered From Geological Report from Exploration Tunnel Paierdorf[7]

γ[kN/m³]	E[MN/m²]	v[-]	c[kN/ m²]	[°]	K_0[-]	Depth z[m]	m[-]
21.5	270	0.2	35	27	0.54	7 0	0.8

In the first step the stiffnessin 70 meter depth is a djusted for the Mohr-Coulombmodel to thelevel of the tunnel axix*z= 30.0*

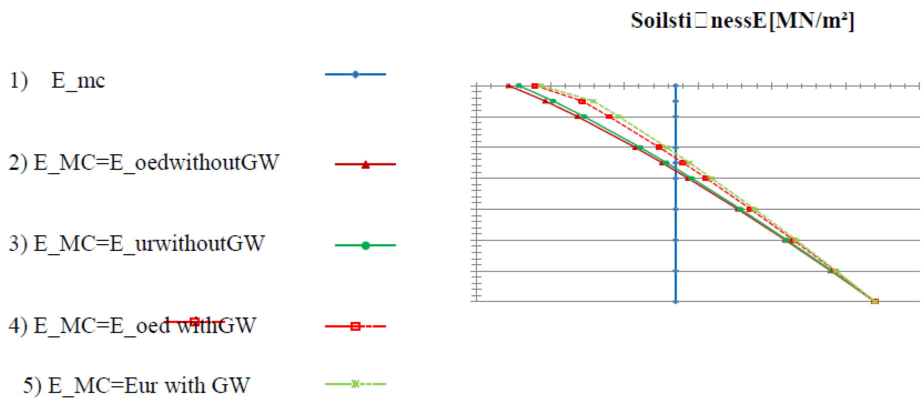

FIGURE 9: Stiffness Parameters

MODEL	$E_{oed,ref}$ [MN/ m²]	$E_{50,ref}$ [MN/ m²]	$E_{ur,ref}$ [MN/ m²]	c[kN/m²]	[°]	M [-]	K_0 [-]	POP [kN /m²]	$K_{0,nc}$ [-]	ur [-]	$G_{0,ref}$ [MN/ m²]	$\gamma_{0,7}$ [-]
1)MC, E135	E=135MN/m²			35	27	-	0.54	-	-	-	-	-
2)HS, $E_{MC}=E_{oed}$	45	45	135	35	27	0.8	0.7	500	0.54	0.2	-	-
3)HS,$E_{MC}=E_{ur}$	20	20	60	35	27	0.8	0.7	500	0.54	0.2	-	-
7)HSS, $E_{MC}=E_{oed}$	45	45	135	35	27	0.8	0.7	500	0.54	0.2	225	$2*10^{-4}$
9)HSS,$E_{MC}=E_{ur}$	20	20	60	35	27	0.8	0.7	500	0.54	0.2	100	$2*10^{-4}$

PARAMETERS FOR DRAINED CALCULATION TABLE 3 : Soil Parameters without Consideration of Ground water

PARAMETERS FOR UNDRAINED CALCULATION TABLE 4: Soil Parameters with Consideration of Groundwater

MODEL	E oed,ref [MN/m²]	E50,ref [MN/m²]	ur,ref [MN/m²]	c [kN/m²]	[°]	m [-]	0[-]	POP [kN/m²]	K 0,nc [-]	Ur [-]	G0,ref [MN/m²]	$\gamma_{0,7}$ [-]
4)HS, $E_{MC}=E_{oed}$	69.3	69.3	207.8	35	27	0,8	0.7	500	0.54	0.2	-	-
5)HS,$E_{MC}=E_{ur}$	30	30	90	35	27	0.8	0.7	500	0.54	0.2	-	-
6)MC, E135	E=135MN/m²			35	27	-	0.54	-	-	-	-	-
8)HSS, $E_{MC}=E_{oed}$	69.3	69.3	207.8	35	27	0.8	0.7	500	0.54	0.2	346.3	2*10-4
10)HSS,$E_{MC}=E_{ur}$	30	30	90	35	27	0.8	0.7	500	0.54	0.2	150	2*10-4

The initial stress state prior to tunnel construction is controlled by the specific weight of the soil [kN/m³], groundwater conditions and many other factors like plate tectonics, weathering and erosion, previous overburden etc. Because of the high number of influencing factors the initial stress distribution is often very difficult to evaluate. In numerical calculations, however, reasonable assumptions regarding the initial stress state are required. [1] In PLAXIS two different methods, Gravity loading and K0-procedure are available to generate the initial stresses. In this thesis only the K0-procedure is used and explained here. The K0- procedure is used to compute initial stresses for situations with a horizontal ground surface and homogeneous or horizontally layered ground. Effective vertical stresses σv' depend on the effective weight of the soil γ' and depth h. Effective horizontal stresses σh' are calculated multiplying the vertical stresses with the coefficient of lateral earth pressure at rest K0. [2] Pore water pressure u is taken into account beneath the ground water table.

$$\sigma 1 = \sigma - u = \gamma . \square - u = (\gamma - \gamma).\square$$
$$\sigma 1 = k\ o\ .\sigma$$

The K0-procedure imposes an initial stress state as a starting point for the numerical analysis. Hence, no deformations are calculated. [2] The history of loading can be considered in PLAXIS by the input of an over-consolidation ratio (OCR) or a pre-overburden pressure (POP) for advanced soil models (HS, HSS, SS, SSC, MCC)

4.1. CONSTANT K0 For a constant K0 the horizontal initial stresses are calculated according to:

$$\sigma 1 = \gamma 1 . z\ [\ k\ N\ \ 3.11\ y\ y\ ,0\ m\ 2\ x\ x\ ,0\ 0\ y\ y\ ,0\ m\ 2$$

Therefore, the horizontal initial stresses at the surface are zero.

4.2. VARIABLE K0 DUE TO LOADING HISTORY (POP) The coefficient of lateral earth pressure in over-consolidated soils is larger than in normally consolidated soil. This effect is automatically taken into account by a variable K0. For the generation of the initial stresses by the K0 procedure in advanced soil models the value of K0 is influenced by k_0^{nc}, ν_{ur}, OCR and POP and is calculated automatically resulting in a stress dependent K0-value [2]

$$k\ n\ c\ .P\ O\ P - v\ u\ r\ .P\ O\ P\ \ k\ = k\ n\ c\ .O\ C\ R\ - v\ u\ r\ .(O\ C\ R\ - 1) + 0\ 1 - v\ u\ r\ \ 3.13\ o\ ,x\ \ o\ \ 1 - v$$

$k\ n\ c$ Coefficient of lateral earth pressure at rest for normally consolidated soils

OCR over-consolidation ratio

POP pre-overburden pressurenb
For this project a POP = 500 kN/m² and a constant K0,x = K0,y = 0.7 is considered.

3.4.3 THE INFLUENCE OF POP ON INITIAL YIELD SURFACES: The position of the volumetric yield surface fc on the p-axis is based on previous stress history. To determine the initial position of the cap-type yield surface PLAXIS needs an equivalent isotropic pre-consolidation stress which is computed using the pre-consolidation stress σp . The pre-consolidation stress σp is based on OCR (over-consolidation ratio) or POP (pre-overburden pressure).

$$OCR = \frac{\sigma_p}{\delta y}$$

$$POP = |\sigma p - \sigma '0 |yy$$

V. SUPPORT MEANS

5.1. MATERIAL PARAMETERS OF THE LINING The primary tunnel lining is made of sprayed concrete. The increase of stiffness with time is considered in a simplified manner by using two different parameter sets for shotcrete young and old. The reduced stiffness of shotcrete young is based on experience to account for distinct creep-properties of the soft shotcrete [9]. The material behaviour is assumed as linearelastic. One calculation phase after excavation the tunnel lining is activated with the material parameter set shotcrete young. In all following phases the properties are changed to shotcrete old. TABLE 5: MATERIAL PARAMETERS LINING

	[kN/m³]	E [MN/m²]	[-]
Shotcrete young	25	4000	0.2
Shotcrete old	25	15000	0.2

5.2. ANCHORS: The shotcrete lining and anchors are the sole support means for the exploratory tunnel.

VI. MESH GENERATION AND QUALITY

6.1. PLAXIS 3D To perform Finite element analysis the model has to be transformed into a Finite element mesh. In PLAXIS 3D 2011 the basic soil elements are 10-noded tetrahedral elements. Structural components are modelled with different types of elements. In the generated model in addition to soil elements only 6-noded plane plate elements are used. [2] FIGURE 17: 10-Noded Tetrahedral Soil Elements (3d) [2] As mentioned above the discretization angle for polylines and the modelled length per slice have a great impact on the shape of the generated elements and therefore the mesh quality. The mesh quality is a factor for the relation of inner to outer sphere of tetrahedral elements. For an ideal tetrahedron it is 1.0. Another parameter to determine the quality of the generated mesh is the target element size or average element size le [2]

6.1.1. INPUT PARAMETERS The following expert settings obtained by trial-and-error were used for the definition of the mesh:
Relative element size factor → 1.5
Polyline angle tolerance → 20°
Surface angle tolerance → 5°
Finess Factors for local refinement of the mesh:
Soil clusters above tunnel → 0.5
Soil clusters around tunnel → 0.1/0. 3
Tunnel cluster → 0.3
Anchor area → 0.1
Plate elements (tunnel lining) → 0.8

6.1.2. GENERATED MESH
The generated mesh consists of 112585 soil elements, 1559789 nodes and has an average element size of 2.302 m

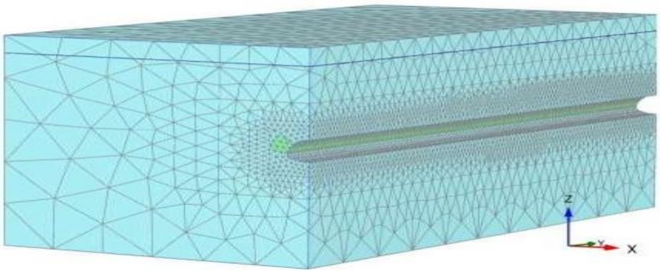

FIGURE 10: 3D Finite Element Mesh

6.2. PLAXIS 2D In PLAXIS 2D the basic soil elements are 15-noded or 6-noded triangular elements. 15-noded elements employ a 4 th order shape function, while 6-noded elements employ only a quadratic shape function. In these calculations 6-noded soil elements are used to achieve compatibility with the 3D calculations. Structural elements have to be compatible with soil elements. When 6-noded soil elements are used plates are modelled with 3-noded plate (line) elements with 3 degrees of freedom per node: two translational degrees of freedom (ux, uy) and one rotational degree of freedom in the x-y plane (φz). For a standard deformation analysis using a plain strain model these elements provided efficient accuracy.

FIGURE 11: 6-noded soil elements (2d)

In 2D the average elements size is calculated from the outer geometry dimensions and the global coarseness factor n_c

$$l_e = \frac{\sqrt{(x_{\max} - x_{\min})(y_{\max} - y_{\min})}}{c}$$

The global coarseness is chosen as coarse (nc = 50) to fit the average element size of the 3D.
The generated mesh consists of 615 soil elements with an average element size of 2.613 m.

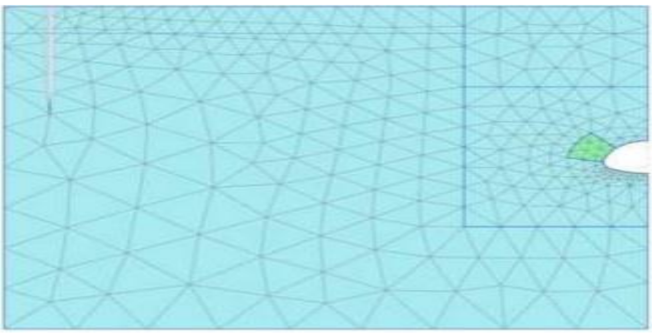

FIGURE 12: 2D Finite Element Mesh

6.7. CONSTRUCTION STAGES FOR 3D CALCULATION

For the 3D staged construction two different calculation scenarios are investigated:
1)“wished-in-place” calculation:
• Excavation, installation of lining with material parameter set “shotcrete old” and activation of the increased cohesion for the anchor area for the entire model length in one phase (used to validate the 3D calculation program by comparison with the 2D WIPcalculation)
2)Step-by-step excavation: Full-face advance for slice i:
• Deactivation of the tunnel cluster (excavation) in slice i
• Activation of the lining (material parameter set “SC young”) in slice i-1
3) Change of material of the anchor area from “Silt” to “Silt + Anchor” in slice i-1

4) Change of the plate material set of the lining to “SC old” in slice i-2

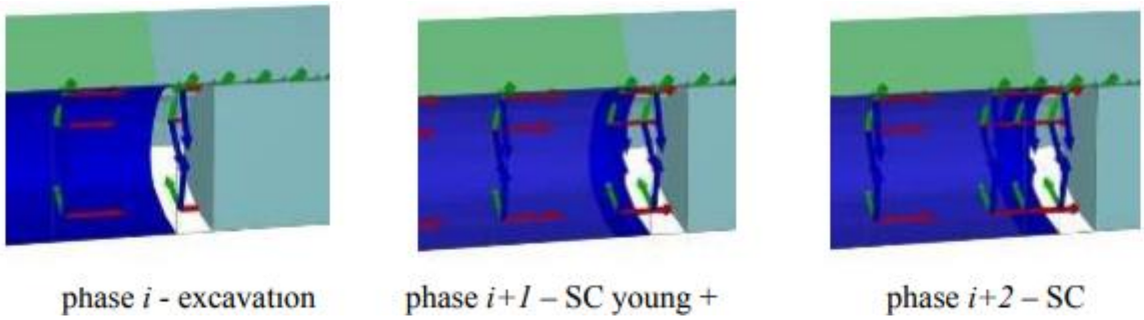

FIGURE 13: Sequential Excavation in 3D

6.8. CONSTRUCTION STAGES FOR 2D CALCULATION

For the 2D calculation two different scenarios are investigated:

1) “wished-in-place” calculation:

- Excavation of the tunnel, installation of the lining with material parameter set “SC old” and activation of the increased cohesion for the anchor area in one step (used to validate the 3D calculation program by comparison with 2D WIP calculation)

2) Sequential excavation:

- Stress-relaxation with ΣMStage< 1.0 in the tunnel cross-section (deactivation of the soil cluster in the tunnel)
- Activation of the lining (material parameter set “SC young”) and change of material of the anchor area from “Silt” to “Silt + Anchor” with ΣMStage<1.0

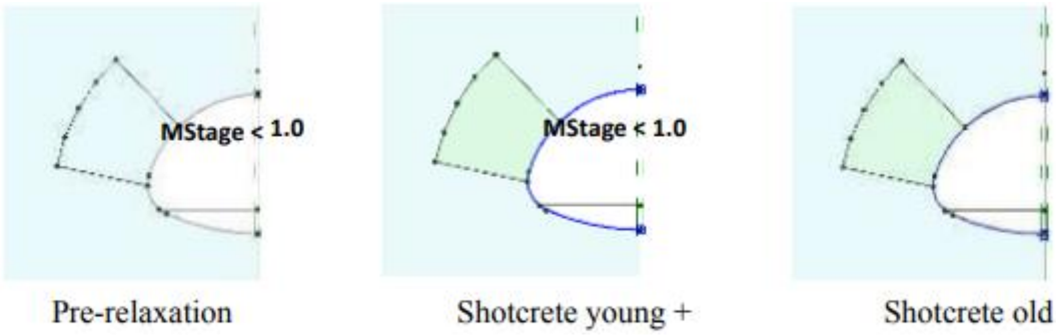

FIGURE 14: Sequential Excavation in 2D

4. WISHED-IN-PLACE” CALCULATIONS IN 2D AND 3D

The major objective of the WIP calculations is to validate the 3D calculation program. WIP calculations are also used to investigate the influence of the initial stress state and small strain stiffness on settlements.

Undrained analyses with the Linear-Elastic (model 11) and the Mohr-Coulomb (model 6) model are carried out to evaluate the distribution of excess pore pressures in longitudinal direction of the tunnel.

4.1. PERFORMED CALCULATIONS

WIP calculations are performed with PLAXIS 2D and PLAXIS 3D for all listed calculation models.

MODEL	$E_{oed,ref}$	$E_{50,ref}$ [MN/m²]	$E_{ur,ref}$ [MN/m²]	c [kN/m]	[°]	m [-]	K_0 [-]	POP [kN/m²]	$K_{0,nc}$	ur [-]	$G_{0,ref}$ [MN/m]	$\gamma_{0,7}$ [-]
1)MC, E135	E = 135 MN/m²			35	27	-	0.54	-	-	-	-	-
2)HS, $E_{MC}=E_{oe}$	45	45	135	35	27	0.8			0.54	0.2	-	-
A							0.7	500				
B							auto	500				
C							0.7	0				
3)HS, $E_{MC}=E_{ur}$	20	20	60	35	27	0.8	0.7	500	0.54	0.2	-	-
7)HSS, $E_{MC}=E_{o}$	45	45	135	35	27	0.8	0.7	500	0.54	0.2	225	2*10
A	Tolerated error = 1.0 % (Standard setting)											
B	Tolerated error = 0.1 %											
9)HSS, EMC=Eu r	20	20	60	35	27	0.8	0.7	500	0.54	0.2	100	2*10

CALCULATIONS WITHOUT GROUNDWATER (DRAINED) TABLE 6: Soil Parameters without Consideration of Groundwater

4.1.2

MODEL	$E_{oed,ref}$ [MN/m²]	$E_{50,ref}$ [MN/m²]	$E_{ur,ref}$ [MN/m²]	c [kN/m²]	[°]	m [-]	K_0 [-]	POP [kN/m²]	$K_{0,nc}$ [-]	ur [-]	$G_{0,ref}$ [MN/m²]	$\gamma_{0,7}$ [-]
4)HS, $E_{MC}=E_{oed}$	69.3	69.3	207.8	35	27	0.8	0.7	500	0.54	0.2	-	-
5)HS, $E_{MC}=E_{ur}$	30	30	90	35	27	0.8	0.7	500	0.54	0.2	-	-
6)MC, E135	E = 135 MN/m²			35	27	-	0.54	-	-	-	-	-
8)HSS, $E_{MC}=E_{oed}$	69.3	69.3	207.8	35	27	0.8	0.7	500	0.54	0.2	346.3	$2*10^{-4}$
A	*Tolerated error = 1.0 % (Standard setting)*											
B	*Tolerated error = 0.1 %*											
10)HSS, $E_{MC}=E_{ur}$	30	30	90	35	27	0.8	0.7	500	0.54	0.2	150	$2*10^{-4}$
11) LE	E = 135 MN/m² ; v' = 0.2											

CALCULATIONS WITH GROUNDWATER (UNDRAINED) TABLE 7: Soil Parameters with Consideration of Groundwater

4.2 SETTLEMENTS

In 3D the deformations are evaluated at the centre of the model (y=71.0 m). The results of 3D FE-analysis are expressed as percentage of the settlements obtained from 2D calculations.

TABLE 8: WIP, Settlements: 1) MC, Drained

	Surface settlements		**Crown settlements**	
PLAXIS 2D	-8.2 mm		-21.3 mm	
PLAXIS 3D	-8.1 mm	98%	-21.2 mm	99%

TABLE 9: WIP, Settlements: 2) HS, Emc = Eoed, Drained

	[mm]	Surface settlements		Surface settlements	
POP500 K_0 =0.7	PLAXIS 2D	-4.6 mm		-10.9 mm	
	PLAXIS 3D	-4.6 mm	99%	-10.8 mm	99%
POP500 K_0 automatic	PLAXIS 2D	-3.3 mm		-9.2 mm	
	PLAXIS 3D	-3.3 mm	101%	-9.1mm	100%
POP0 K_0 =0.7	PLAXIS 2D	-7.0 mm		-13.4 mm	
	PLAXIS 3D	-7.0 mm	100%	-13.3 mm	100%

TABLE 10: WIP, Settlements: 3) HS, Emc = Eur, Drained

	Surface settlements		Crown settlements	
PLAXIS 2D	-9.1 mm		-21.7 mm	
PLAXIS 3D	-9.0 mm	*98%*	-21.5 mm	*99%*

TABLE 11: WIP, Settlements: 4) HS, Emc = Eoed, Undrained

	Surface settlements		Crown settlements	
PLAXIS 2D	-3.0 mm		-7.4 mm	
PLAXIS 3D	-2.7 mm	*90%*	-6.7 mm	*90%*

TABLE 12: WIP, Settlements: 5) HS, Emc = Eur, Undrained

	Surface settlements		Crown settlements	
PLAXIS 2D	-5.8 mm		-14.1 mm	
PLAXIS 3D	-5.5 mm	95%	-13.6 mm	96

TABLE 13: WIP, Settlements: 6) MC, Undrained

	Surface settlements		Crown settlements	
PLAXIS 2D	-5.9 mm		-13.9 mm	
PLAXIS 3D	-5.6 mm	*96%*	-13.5 mm	*97%*

TABLE 14: WIP, Settlements: 7) HSS, Emc = Eoed, Drained

	Surface settlements		Crown settlements	
PLAXIS 2D	-1.7 mm		-4.3 mm	
PLAXIS 3D tol.error 0.01	-1.7 mm	*98%*	-4.2 mm	*99%*
PLAXIS 3D tol.error 0.001	-1.7 mm	*99%*	-4.3 mm	*99%*

TABLE 15: WIP, Settlements: 8) HSS, Emc = Eoed, Undrained

	Surface settlements		Crown settlements	
PLAXIS 2D	-1.4 mm		-3.4 mm	
PLAXIS 3D tol. error 0.01	-1.2 mm	*85%*	-3.1 mm	*90%*
PLAXIS 3D tol. error 0.001	-1.2 mm	*86%*	-3.1 mm	*91%*

TABLE 16: WIP, Settlements: 9) HSS, Emc = Eur, Drained

	Surface settlements		**Crown settlements**	
PLAXIS 2D	-3.5 mm		-9.1 mm	
PLAXIS 3D tol.error 0.001	-3.5 mm	*99%*	-9.0 mm	*99%*

TABLE 17: WIP, Settlements: 10) HSS, Emc = Eur, Undrained

	Surface settlements		**Crown settlements**	
PLAXIS 2D	-2.6 mm		-6.3 mm	
PLAXIS 3D tol.error 0.001	-2.3 mm	*91%*	-6.0 mm	*94%*

The settlements obtained from 2D and 3D computation are in good agreement. Differences in undrained analysis are generally larger than in drained analysis when using the Hardening Soil and HS-small model. Except for calculation model 8) all results are within a 10 %-range.

4.2.1. INFLUENCE OF THE INITIAL STRESS STATE

Settlements obtained from calculations with POP = 0 kN/m² are expected to be larger than for calculations with POP = 500 kN/m² and K0 = 0.7. Smallest settlements should result from calculation with POP = 500 kN/m² and an automatically calculated K0.

4.2.2. INFLUENCE OF SMALL-STRAIN STIFFNESS

The influence of small strain stiffness on the development of settlements is investigated by comparing the corresponding calculation with the Hardening Soil and HS-small model.

TABLE 18: WIP: Hardening Soil Vs. HS-Small

		Hardening Soil	**Hardening Soil-small**
Drained	$E_{MC} = E_{oed}$	2)	7)
	$E_{MC} = E_{ur}$	3)	9)
Undrained	$E_{MC} = E_{oed}$	4)	8)
	$E_{MC} = E_{ur}$	5)	10)

Due to increased stiffness at small strains settlement computed with the HS-small model are expected to be smaller than settlements obtained from calculations with the corresponding Hardening Soil model.

The small-strain shear modulus G0 is 4-times higher than the un-/reloading shear stiffness Gur. With increasing strains the initial stiffness decreases until it reaches Gur (Eur respectively). At G/Gur the model switches to the hardening plasticity of the Hardening Soil model.

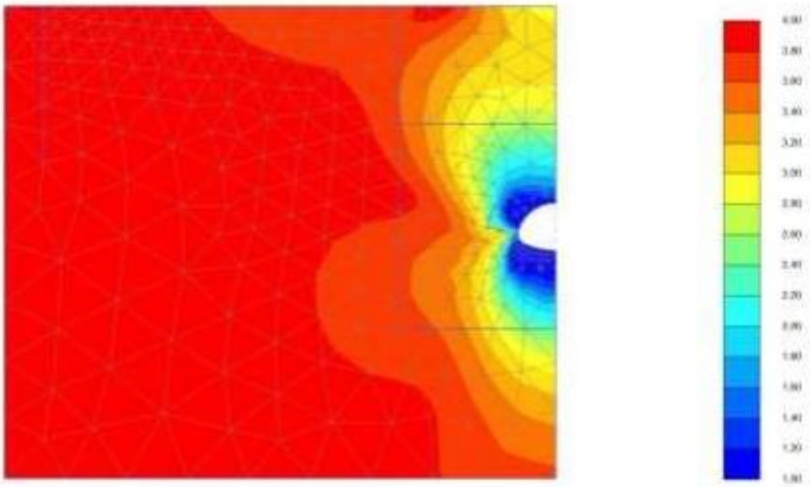

FIGURE 15: Ratio G/ Gur for Drained "Wished-In-Place" Computations Using the HS-Small Model (Plaxis 2D)

TABLE 19: Ratio Of "Wished-In-Place" Settlements: Hardening Soil Vs. HS-Small (Emc=Eoed)

		surface	crown
Drained 2) and 7)	2D	2.7	2.5
	3D	2.7	2.5
Undrained 4) and 8)	2D	2.1	2.2
	3D	2.3	2.3

TABLE 20: Ratio Of "Wished-In-Place" Settlements: Hardening Soil Vs. HS-Small (Emc=Eur)

		surface	crown
Drained 3) and 9)	2D	2.6	2.2
	3D	2.6	2.2
Undrained 5) and 10)	2D	2.1	2.1
	3D	2.4	2.3

The influence of small-strain stiffness is, therefore, higher for surface settlements. The lower stiffness results in a smaller influence of small-strain stiffness. The ratio of surface and crown settlements obtained from HS and HSS calculations are the same.

4.4. DISTRIBUTION OF EXCESS PORE PRESSURES IN UNDRAINED ANALYSIS

Undrained analyses with the Linear-Elastic (model 11) and the Mohr-Coulomb (model 6) model are used to evaluate the distribution of excess pore pressures in longitudinal direction of the tunnel. The nodal values of excess pore pressure are compared for different y - values in 3 nodes

- point A – tunnelshoulder
- point B – tunnel springline
- point C – tunnel invert

4.4.1. LINEAR-ELASTIC MODEL : To evaluate the source of inconsistencies a calculation with the Linear-Elastic model is performed. Influences of lining installation and water conditions in the tunnel are investigated.

TABLE 21: Versions for "Wished-In-Place" Calculation Using Linear-Elastic Model.

	Tunnel lining	Water conditions for the tunnel cluster
Calculation 1	yes	dry
Calculation 2	no	dry
Calculation 3	no	Phreatic level

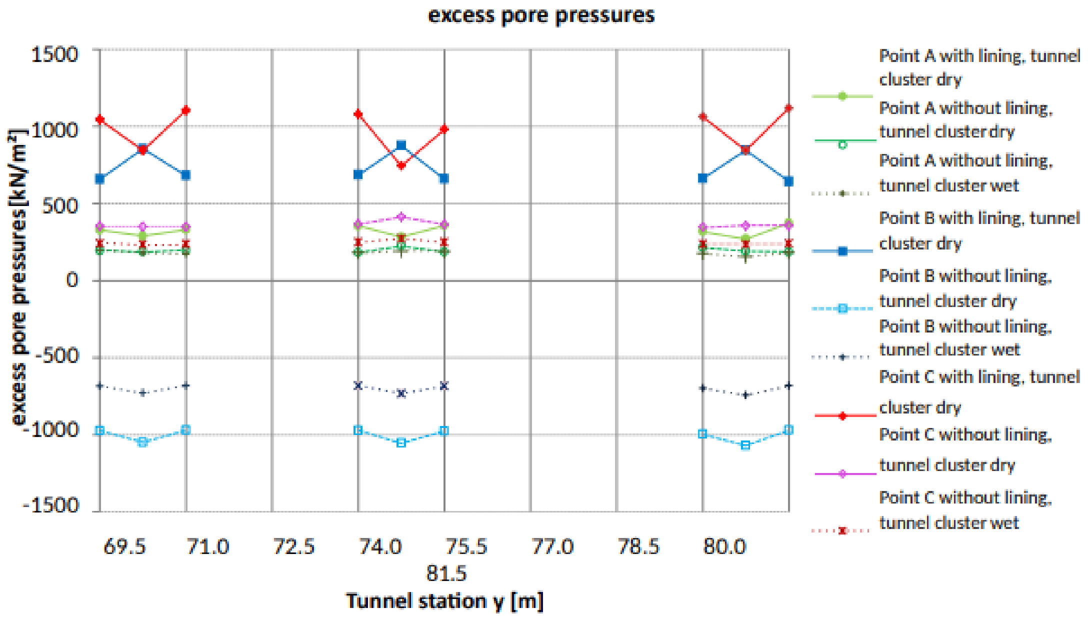

FIGURE 16: LE, WIP: Distribution Excess Pore Pressures Over Tunnel Length

At the junction between tunnel, anchor area and the ground the largest differences occur. Linear-elastic soil behaviour is assumed to evaluate the influence of lining installation.

4.1.2. MOHR-COULOMB MODEL

The nodal values of excess pore pressure are also compared for an undrained Mohr-Coulomb analysis for 4 excavation lengths between station 63.5 and 91.5 m in the middle of the FE-model.

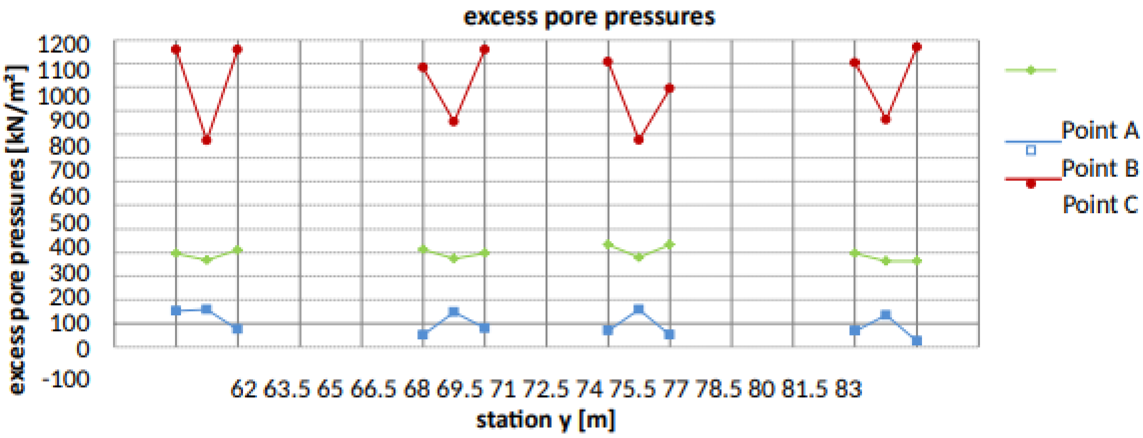

FIGURE 17: MC, Undrained, WIP: Distribution Excess Pore Pressures Over Tunnel Length

4.4.3. HARDENING SOIL AND HS-SMALL MODEL In undrained analysis with the Hardening Soil model and HS-small model negative excess pore pressures are generated at the tunnel springline and positive excess pore pressures at the tunnel crown and invert. In the figures below the results of 2D WIP calculations are compared.

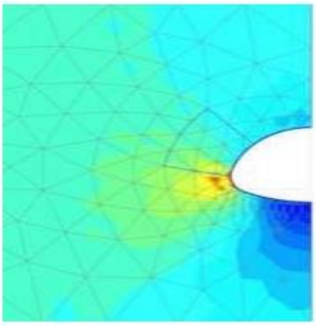

FIGURE 33: 2D : 5) HS, UNDRAINED, WIP: EXCESS PORE PRESSURE

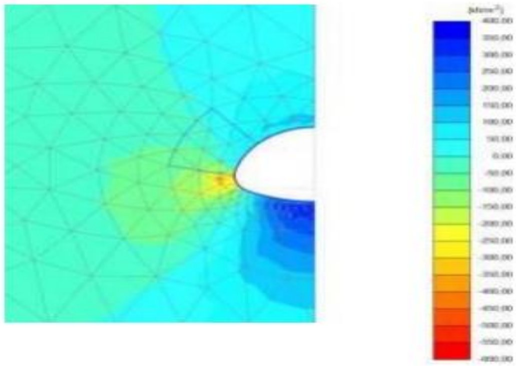

FIGURE 34: 2D : 10) HSS UNDRAINED, WIP: EXCESS PORE PRESSURE

5. DRAINED 3D CALCULATIONS

Drained analyses are performed without consideration of groundwater conditions due to insufficient ground stability as explained in chapter 3.3. To overcome boundary conditions a 20 m "wished-in-place" section is inserted at the beginning and the end of the model.

5.1. PERFORMED CALCULATIONS

TABLE 23: Soil Parameters Without Consideration of Groundwater

MODEL	$E_{oed,ref}$ [MN/m²]	$E_{50,ref}$ [MN/m²]	$E_{ur,ref}$ [MN/m²]	c [kN/m²]	[°]	m [-]	K_0 [-]	POP [kN/m²]	$K_{0,nc}$ [-]	ur [-]	$G_{0,ref}$ [MN/m²]	$\gamma_{0,7}$ [-]
1)MC, E135	E=135 MN/m²			35	27	-	0.54	-	-	-	-	-
2)HS, E_{MC}=E_{oed}	45	45	135	35	27	0.8	0.7	500	0.54	0.2	-	-
A							0.7	500				
B							auto	500				
C							0.7	0				
3)HS, E_{MC}=E_{ur}	20	20	60	35	27	0.8	0.7	500	0.54	0.2	-	-
7)HSS, E_{MC}=E_{oed}	45	45	135	35	27	0.8	0.7	500	0.54	0.2	225	$2*10^{-4}$
A	*Tolerated error = 1.0 % (Standard setting)*											
B	*Tolerated error = 0.1 %*											
9)HSS, E_{MC}=E_{ur}	20	20	60	35	27	0.8	0.7	500	0.54	0.2	100	$2*10^{-4}$

5.2. INFLUENCE OF TOLERATED ERROR IN HS-SMALL CALCULATIONS

When using the Hardening-Soil model with small strain stiffness for computation of sequential tunnel excavation the out-of-balance force at the tunnel face has to be checked At the tunnel face the total stresses in longitudinal direction σyy have to be around zero to be in equilibrium. In any non-linear analysis with a finite number of calculation steps no exact solution is reached. It has to be ensured that the error remains in acceptable bounds.

The global error is related to the sum of out-of-balance nodal forces. The local error refers to the error at each stress point. If the local error exceeds the Tolerated error the stress point is defined as inaccurate plastic point. The number of inaccurate points is limited. The global error has to be lower than the Tolerated error. [2]

□□□□□□□□□□□□□ □□□□□□□□□□□ = ∑‖□□□□□□□ □□□□ □□□□□□□□□□□□□□□ □□□□□□□□□□ □□□□□□□□□□□□□□‖ ≤ □□□□□□□□□□□□□□□□□□□□□ □□□□□□□□□□□
∑‖□□□□□□□□□□□□□ □□□□□□□□□□□‖

5.3. SURFACE SETTLEMENTS

Surface settlements are evaluated after completed tunnel construction in two nodes in the middle of the FE- model above the tunnel centre-line. -Node 1: 0.0/71.0/0.0 & Node 2:0.0/74.23/0.0.

5.3.1. TRANSVERSAL SETTLEMENT TROUGH The corresponding transversal settlement troughs in Station y = 71.0 m are displayed in Figure 36. They are compared to field measurements at station MQ 1015, 1040, 1067 and 1146

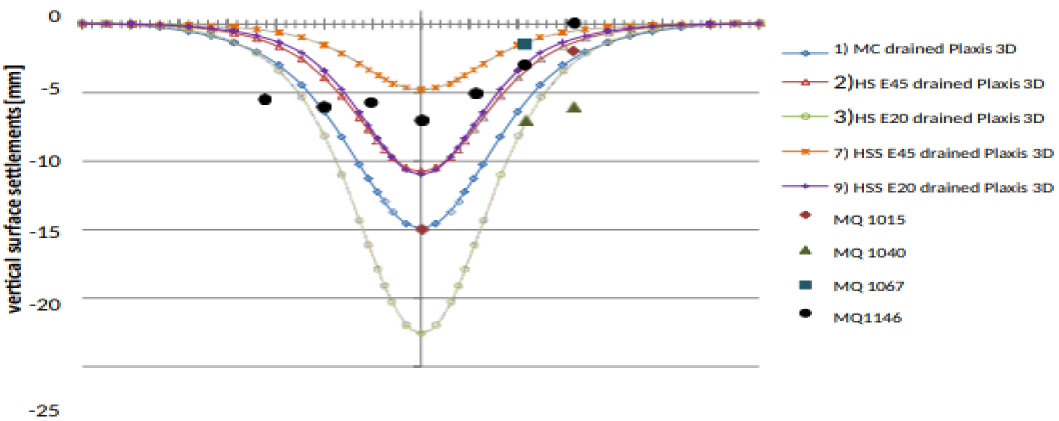

FIGURE 18: Comparison of The Transversal Surface Settlement Trough at Station 1015, 1040, 1067 And 1146 With the Results of The Numerical Drained Calculations in Station 71

5.3.2. LONGITUDINAL SETTLEMENT PROFILE

In Figure 37 the longitudinal settlement profile for station 71.0 m over the position of the advancing tunnel face is displayed. It is compared to field measurements in station 1015 and 1146.

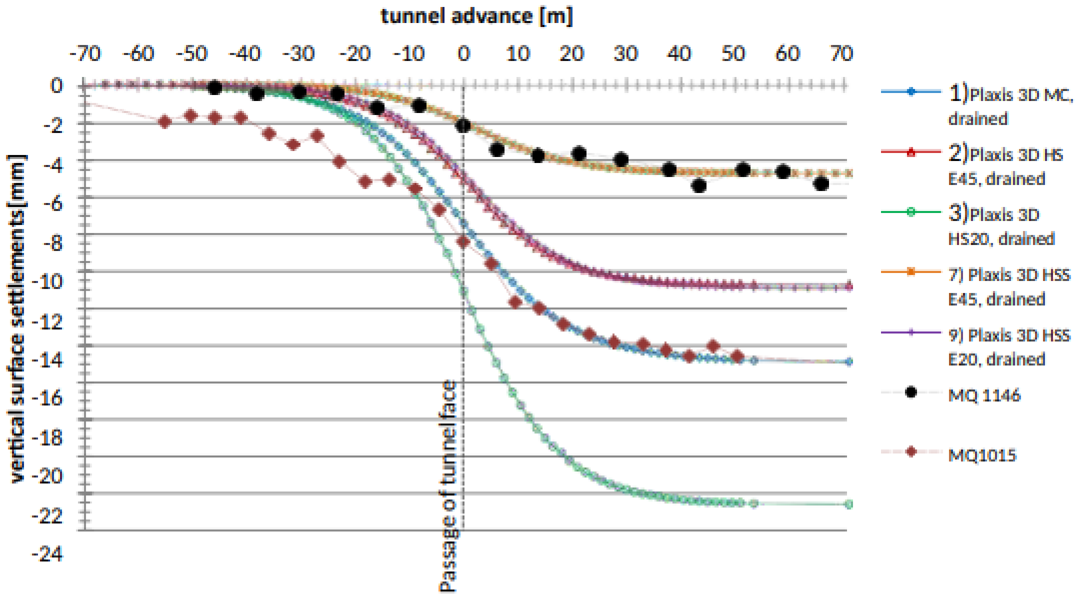

FIGURE 19: Comparison of The Development of Surface Settlements at Station 1015 And 1146 With the Results of The Numerical Drained Calculations in Station 71

5.4. LINING FORCES AND DEFORMATIONS

5.4.1. CROWN SETTLEMENT Crown settlements are evaluated after completed tunnel construction at the beginning, end and centre of one excavation length in the middle of the FE-model. The vertical settlements obtained from the three-dimensional numerical calculations are summarized in Table 25.

TABLE 25: Crown Settlements from Drained FE-Analysis

	Eoed,ref [MN/m²]	E50,ref [MN/m²]	Eur,ref [MN/m²]	station		
				74.00 m	74.75 m	75.50 m
1) MC	E=135 MN/m²			-36 mm	-39 mm	-36 mm
2A) HS E45	45	45	135	-27 mm	-32 mm	-27 mm
2B) HS E45				-26 mm	-31 mm	-26 mm
2C) HS E45				-29 mm	-33 mm	-27 mm
3) HS E20	20	20	60	-56 mm	-67 mm	-56 mm
7) HSS E45	45	45	135	-17 mm	-21 mm	-17 mm
9) HSS E20	20	20	60	-41 mm	-52 mm	-41 mm

The crown settlements range from -17 to -56 mm. The largest settlements are obtained from calculations with EMC = Eur. When considering small-strain stiffness smaller deformations are calculated compared to the corresponding standard HS model.

5.4.2. LINING FORCES

The axial forces and bending moments in the lining are displayed in the figures below. Table 27 summarises the minimum and maximum values. Due to the discretization of the curved tunnel circumference with straight lines and tetrahedral elements no smooth distribution of internal forces is obtained.

TABLE 27: INTERNAL LINING FORCES

		1)MC	2)HS $E_{MC}=E_{oed}$	3)HS $E_{MC}=E_{ur}$	7)HSS $E_{MC}=E_{oed}$	9)HS $E_{MC}=E_{ur}$
M [kNm/m]	min	-54	-31	-43	-18	-30
	max	59	37	65	19	39
N [kN/m]	min	356	481	481	410	484
	max	793	817	851	624	741

The minimum axial forces occur at the tunnel crown, the maximum values at the tunnel springline. Compared to the Hardening Soil and HS-small model, the Mohr Coulomb model predicts the smallest values at the crown. The consideration of small-strain stiffness leads to a reduction of maximum axial forces by 10 – 20 %

6. UNDRAINED 3D CALCULATIONS

6.1. MODELLING UNDRAINED BEHAVIOUR IN PLAXIS

An undrained analysis is required when the permeability of the soil is low, the rate of loading is high and short term behaviour has to be assessed [12]. According to Terzaghi's principle the pore water pressure contributes to the total stress level in the soil body.

$$\sigma_{tot} = \sigma^{1} + \sigma_{\omega}$$

In PLAXIS three different drainage types for undrained analysis are possible.

1) Undrained (A): Undrained effective stress analysis with effective strengthparameters
2) Undrained (B): Undrained effective stress analysis with undrained strength parameters
3) Undrained (C): Undrained total stress analysis with undrained parameters

In the following calculation method A was chosen for undrained analysis. Method A uses effective strength parameters to calculate the undrained shear strength cu.

6.2. PERFORMED CALCULATIONS

The groundwater table lies 5.0 m below the surface. The steady state pore pressures are generated using the phreatic level. This results in a maximum water pressure at the model bottom.

MODEL	$E_{oed,ref}$ [MN/m²]	$E_{50,ref}$ [MN/m²]	$E_{ur,ref}$ [MN/m²]	c [Kn/m²]	[°]	m [-]	K0 [-]	POP [kN/m²]	K0,nc [-]	ur [-]	G0,ref [MN/m²	γ0,7 [-]
4)HS, E_{MC} = = E_{oed}	69.3	69.3	207.8	35	27	0.8	0.7	500	0.54	0.2	-	-
C1	Consolidation phase after completed tunnel construction (100 days)											
C2	Tunnel construction during consolidation											
5)HS , E_{MC} = E_{UR}	30	30	90	35	27	0.8	0.7	500	0.54	0.2	-	-
C1	Consolidation phase after completed tunnel construction (100 days)											

6)M C, E135	E=135 MN/m²		35	27	-	0.54	-	-	-	-	-	
C1	Consolidation phase after completed tunnel construction (100 days)											
C2	Tunnel construction during consolidation											
C3	Consolidation phase after every plastic, staged construction phase											
8)HSS, $E_{MC} = E_{oed}$	69.3	69.3	207.8	35	27	0.8	0.7	500	0.54	0.2	346.3	49^{2*1}
A	Tolerated error = 1.0 % (Standard settings)											
B	Tolerated error = 0.1 %											
C1	Consolidation phase after completed tunnel construction (100 days)											
10)H SS, $E_{MC} = E_{UR}$	30	30	90	35	27	0.8	0.7	500	0.54	0.2	150	^{2*1} 0-4

6.3. INFLUENCE OF TOLERATED ERROR IN HS-SMALL CALCULATIONS As for drained analysis the equilibrium stress field in longitudinal direction at the tunnel face is checked. For tunnelling under undrained conditions below the phreatic level the water pressure at the tunnel face has to be considered. The total longitudinal stresses have to be in equilibrium. Negative stresses σyy are generated independent of the constitutive model and the Tolerated error used.

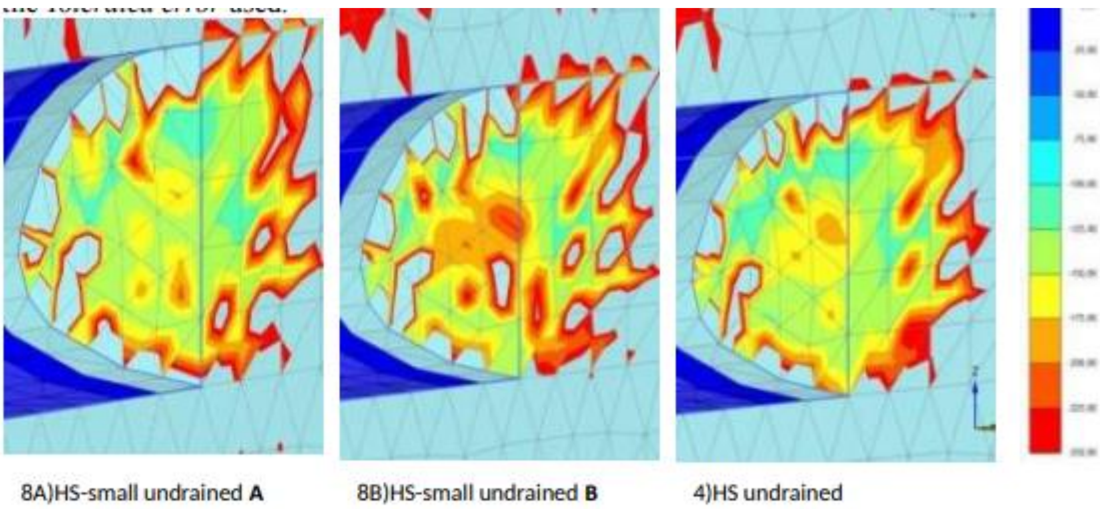

FIGURE 19: Longitudinal Total Stresses at the Tunnel Face under Undrained Conditions

6.4. SURFACE SETTLEMENTS
Surface settlements are evaluated after completed tunnel construction in two nodes in the middle of the FE- model above the tunnel centre-line.
-Node 1: 0.0/71.0/0.0
– Node 2: 0.0/74.23/0.0
The vertical settlements obtained from the three-dimensional numerical calculations are summarized in Table 29

TABLE 29: SURFACE SETTLEMENTS FROM UNDRAINED FE-ANALYSIS

	Eoed,ref [MN/m²]	E50,ref [MN/m²]	Eur,ref [MN/m²]	position 71.00 m	position 74.23 m
4) HS E69	69	69	208	-8 mm	-8 mm
5) HS E30	30	30	90	-16 mm	-16 mm
6) MC	E=135 MN/m²			-12 mm	-12 mm
8) HSS E69	69	69	208	-4 mm	-4 mm
10) HSS E30	30	30	90	-11 mm	-11 mm

Settlements obtained from undrained analysis are generally smaller compared to the results of the corresponding drained analysis.

1. TRANSVERSAL SETTLEMENT TROUGH The corresponding transversal settlement troughs in Station y = 71.0 m are displayed in Figure 44. The numerical results are compared to field measurements at station MQ 1015, 1040, 1067 and 1146.

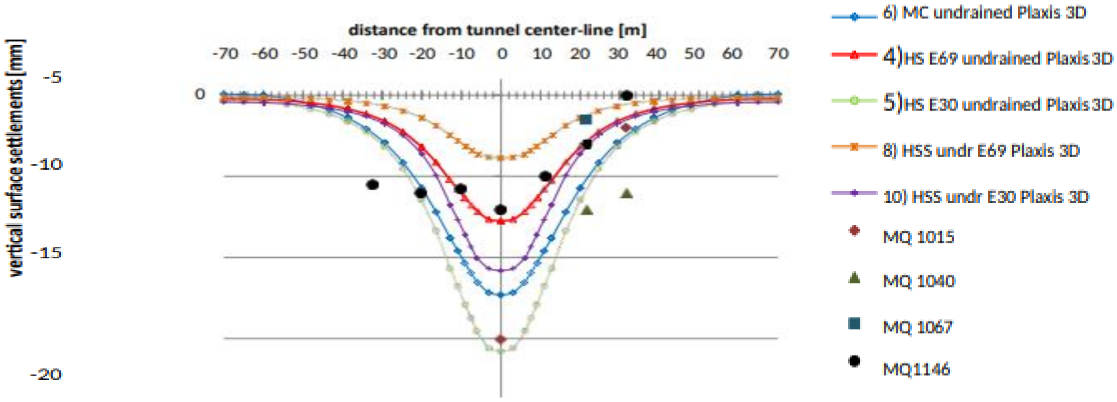

FIGURE 20: Comparison of the Transversal Surface Settlement Trough at Station 1040, 1067 and 1146 with the Results of the Numerical Undrained Calculations in Station 71

Settlements calculated in undrained analysis are generally smaller than the deformations obtained from comparable drained analysis. Unlike in drained analysis the softer HS-small model 10) results in a significantly deeper settlement trough than the stiffer HS model.

Settlements obtained from calculations using the standard Hardening Soil model are 2.4-times larger than corresponding deformations computed with the HS- small model.

2.LONGITUDINAL SETTLEMENT PROFILE

In Figure 45 the longitudinal settlement profile for station 71.0 m over the position of the advancing tunnel face is displayed. It is compared to field measurements in station 1015 and 1146.

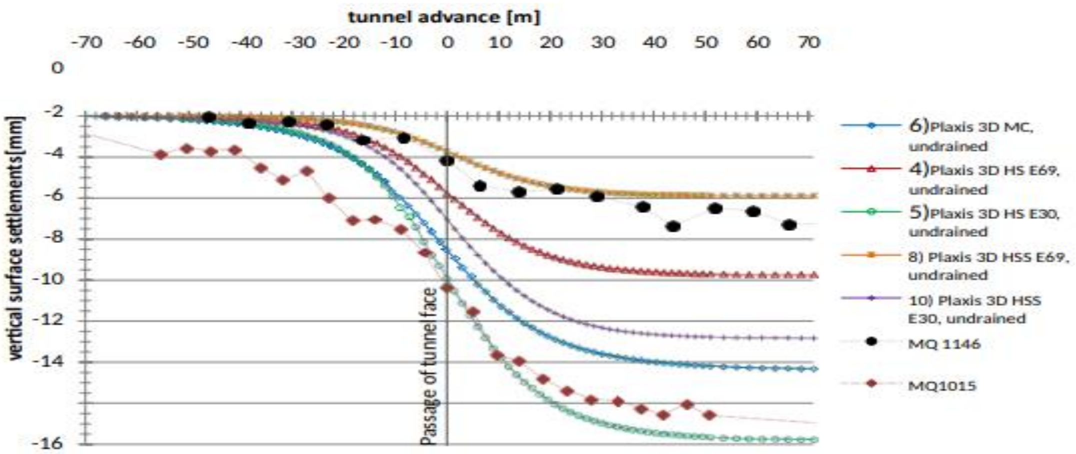

FIGURE 21: Comparison Of The Development Of Surface Settlements At Station 1015 And 1146 With The Results Of The Numerical Undrained Calculations In Station 71

6.5. LINING FORCES AND DEFORMATIONS

1. CROWN SETTLEMENTS Crown settlements are evaluated after completed tunnel construction at the beginning, end and centre of one excavation length in the middle of the FE-model. The vertical settlements obtained from the three-dimensional numerical calculations are summarized in Table 30

TABLE 30: CROWN SETTLEMENTS FROM UNDRAINED FE-ANALYSIS

	Eoed,ref [MN/m²]	E50,ref [MN/m²]	Eur,ref [MN/m²]	station		
				74.00	74.75	75.50
4) HS E69	69	69	208	-20 mm	-21 mm	-20 mm
5) HS E30	30	30	90	-40 mm	-42 mm	-39 mm
6) MC	E=135 MN/m²			-28 mm	-29 mm	-28 mm
8) HSS E69	69	69	208	-10 mm	-10 mm	-10 mm
10) HSS E30	30	30	90	-27 mm	-28 mm	-27 mm

Settlements obtained from undrained analysis are generally smaller than settlements resulting from drained calculations due to the incompressibility of pore water. Furthermore, it reduces the sagging of the tunnel crown.

In Table 31 the difference between predicted crown settlements at the time of the passage of the tunnel face and steady state crown settlements is shown. The pre-displacements are expressed as percentage of steady state deformations.

TABLE 31: Difference between Crown Settlements at the Passage of the Tunnel Face and Steady State Crown Settlements

	Passage of the tunnel face		*Steady state*	*difference*
6) MC undrained	-18.6 mm	66%	-28.2 mm	-9.6 mm
4) HS E69 undrained	-12.4 mm	62%	-20.2 mm	-7.7 mm
5) HS E30 undrained	-26.1 mm	65%	-40.2 mm	-14.1 mm
8) HSS E69 undrained	-5.8 mm	58%	-10.0 mm	-4.2 mm
10) HSS E30 undrained	-18.1 mm	66%	-27.3 mm	-9.2 mm
MQ 1044	0.0 mm		-19.5 mm	-19.5 mm
MQ 1176	0.0 mm		-9.0 mm	-9.0 mm

At station 1044 the maximum measured settlement is -19.5 mm, in station 1176 it is -9.0 mm. The results of undrained numerical calculation vary depending on the model and the parameter set between -4.2 and -14.1 mm, lying in the range of the measurements.

2.LINING FORCES

The axial forces and bending moments in the lining are displayed in the figures below. Table 32 summarizes the minimum and maximum values. Internal lining forces obtained from calculations with PLAXIS 3D 2011 have to be evaluated carefully. Due to the discretization of the curved tunnel circumference with straight lines and tetrahedral elements no smooth distribution in the 3D FE-calculations of internal forces is obtained.

TABLE 32: Internal Lining Forces (Undrained Analysis)

		6)MC	**4)HS $E_{MC}=E_{oed}$**	**5)HS $E_{MC}=E_{ur}$**	**8)HSS $E_{MC}=E_{oed}$**	**10)HS $E_{MC}=E_{ur}$**
M [kNm/m]	*min*	-35	-24	-38	-13	-23
	max	43	30	43	19	30
N [kN/m]	*min*	546	585	656	461	493
	max	955	982	1159	892	1263

In undrained analysis no general statement about the influence of different soil models can be made. The magnitude of internal lining forces depends on the used soil stiffness parameters and generated excess pore pressures.

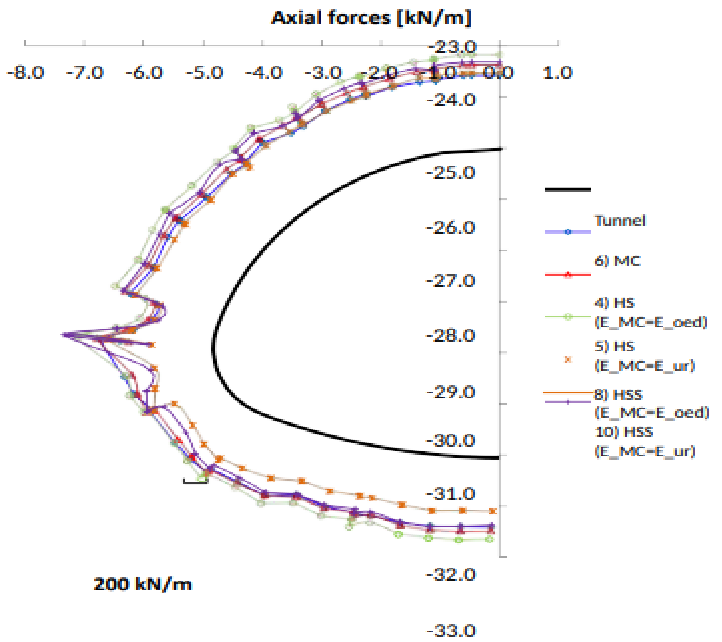

FIGURE 22: Axial Forces (Undrained Analysis)

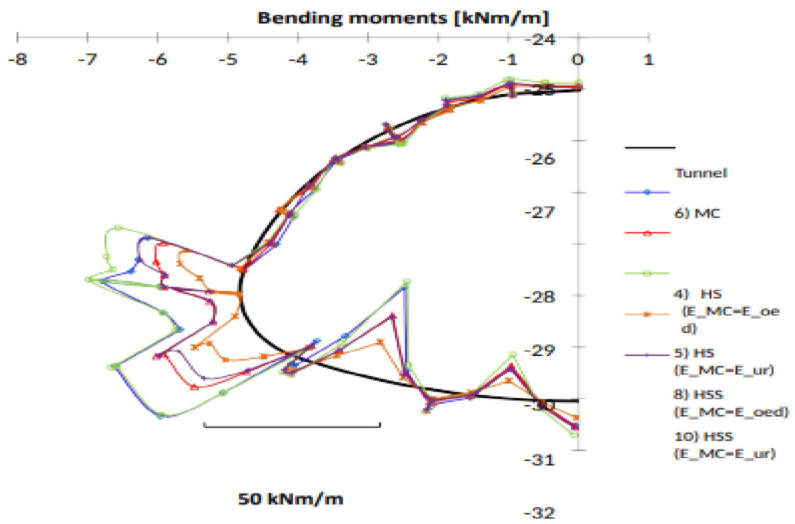

FIGURE 23: Bending Moments (Undrained Analysis)

7. COMPARISON WITH ANALYTICAL METHODS

For a single tunnel in “green-field-conditions” the development of the surface settlements can be described by a Gaussian distribution.

7.1. TRANSVERSAL SURFACE SETTLEMENT TROUGH

Peck [17] was the first to show, that the shape of the transverse settlement trough immediately after tunnel construction is well described by a Gaussian distribution curve

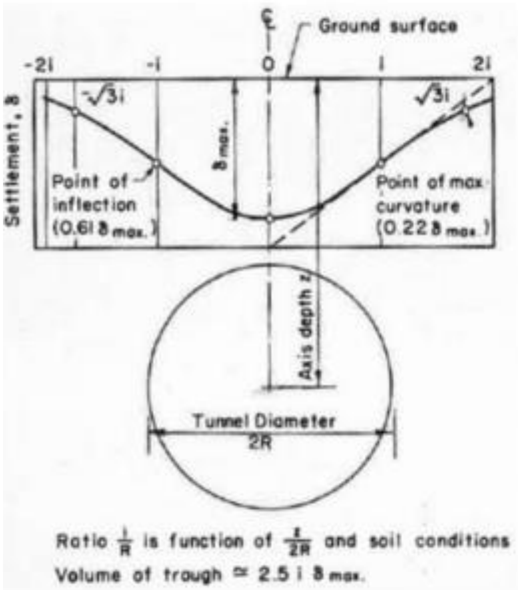

FIGURE 51: Gaussian distribution Curve for Transverse Surface Settlement Profile

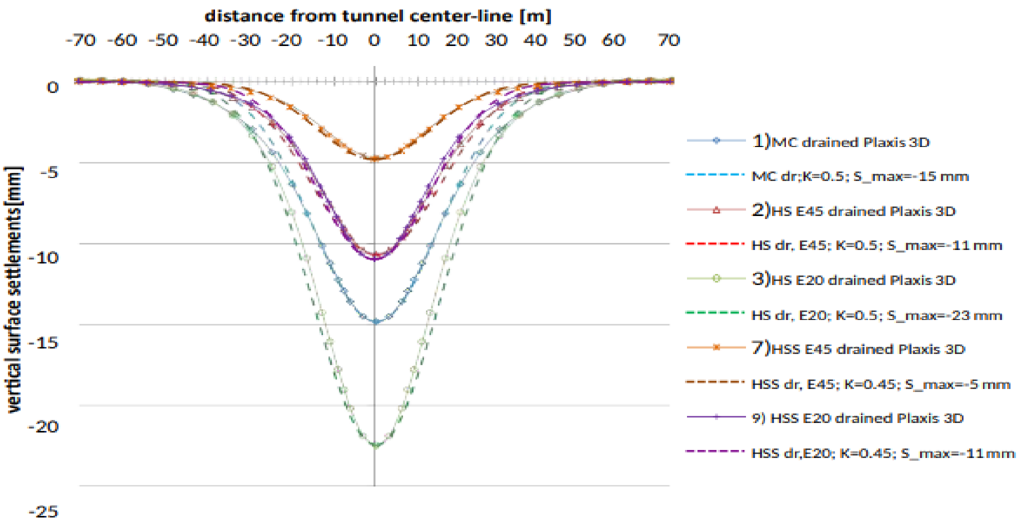

FIGURE 24: Transversal Settlement Trough for Drained Analysis

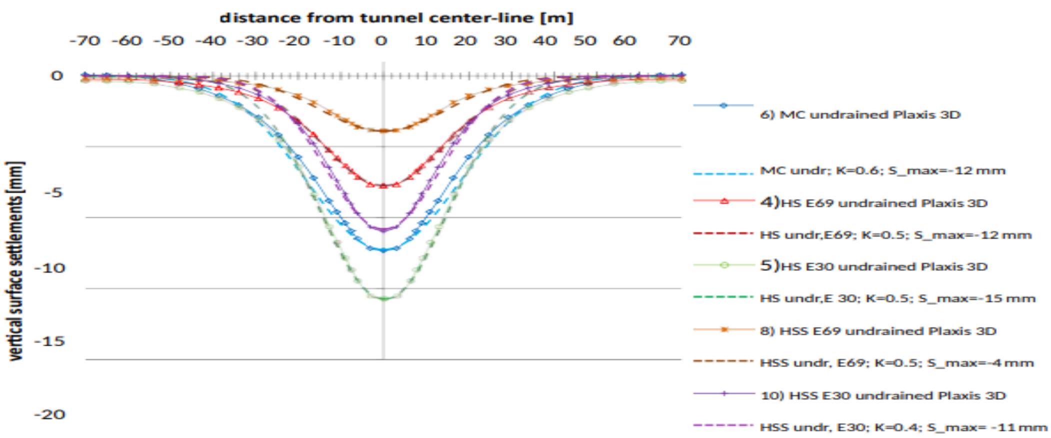

Figure 25: Transversal Settlement Trough for Undrained Analysis

The shape of the surface settlement trough obtained from FE-analysis is matched quite by the Gaussian distribution curve with a width parameter K = 0.5. Generally undrained analysis leads to a wider surface settlement trough. Consideration of small-strain stiffness results in a narrower and Steeper Settlement Trough And Is Better Matched Using A Width Parameter K = 0.45 For Drained Analysis. In Undrained Analysis The Settlement Profiles Resulting From Calculations With The Hardening Soil Model Are Wider Than Predicted By The Gaussian Distribution Curve.

For FE-analysis with the Hardening Soil model the influence of the initial stresses on the development of the transversal surface settlement trough is investigated and the trough width parameter is adapted to match numerical calculation.

7.2. LONGITUDINAL SURFACE SETTLEMENT TROUGH

Beside the transversal settlement profile, the development of the longitudinal surface settlement trough is important for the prediction of three-dimensional influences of settlements on structures close or directly above the tunnel axis. . Attwell and Woodman [18] concluded from several field studies that the longitudinal settlement trough above the tunnel centre line follows a cumulative probability function.

The calculation of the longitudinal surface settlement profile with the cumulative probability function according to Attwell and Woodman [18] over-predicts the surface settlements ahead of the tunnel face. The undrained analysis using the Hardening Soil model is the best fitting of the theoretical distribution

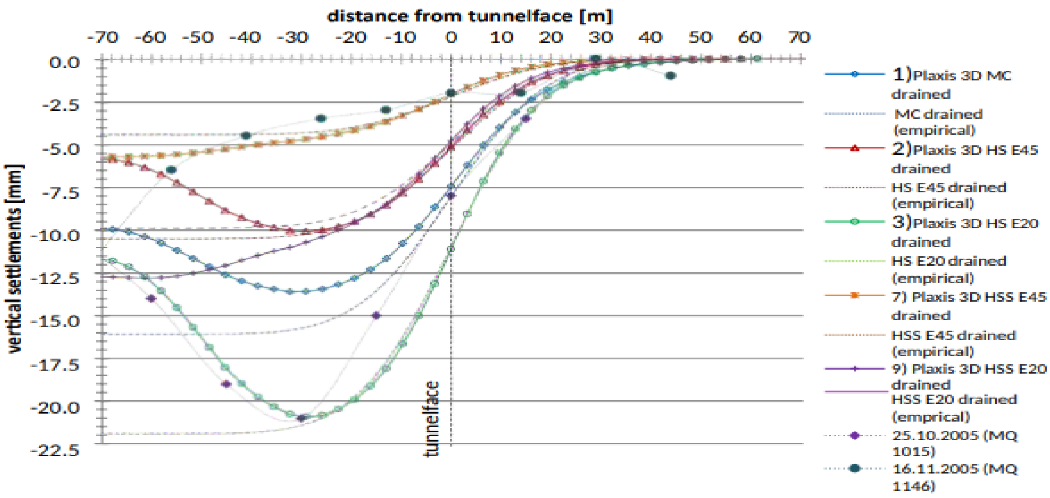

FIGURE 26: Longitudinal Surface Settlement Trough for Drained Analysis

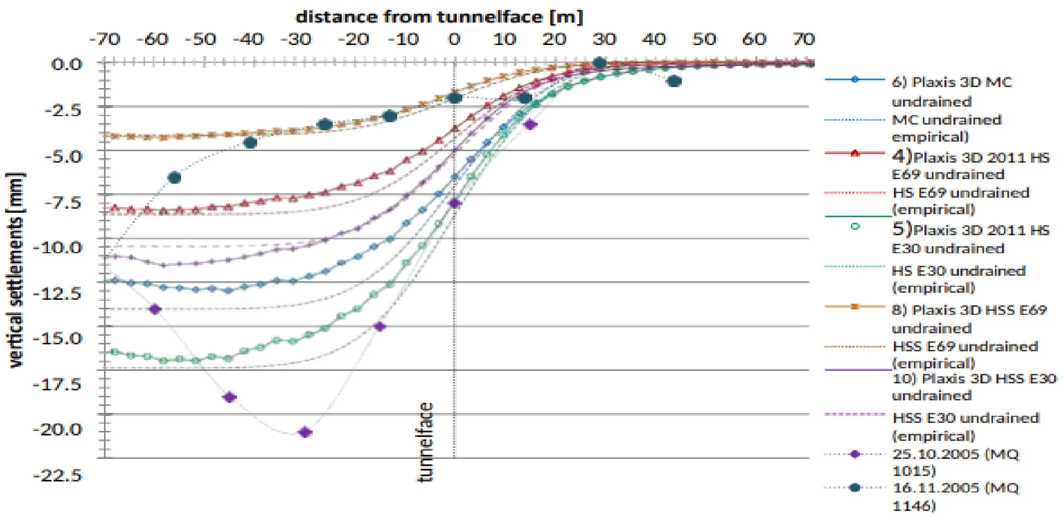

FIGURE 27: Longitudinal Surface Settlement Trough for Undrained Analysis

The influence of the initial stress distribution on the development of the longitudinal settlement trough corresponds to the influence on the transversal settlement profile. For undrained analyses the cumulative probability curves are a better fit to the longitudinal surface settlement profile in 3D due to sequential excavation also at the tunnel start.

8. CONCLUSION

The objective of this thesis was to compare 3D and 2D FE-analysis and empirical methods for the assessment of tunnel induced settlements and internal lining forces. The influence of different reference values, constitutive models and the initial stress state was of main interest.

The investigated tunnel "Mitterpichling Ost" is an exploratory tunnel with a non-circular cross section. It is excavated as the top heading of the final tunnel using the New Austrian Tunnelling Method. Although ground conditions were assumed homogenous, field measurements of deformations showed a wide scatter. All used soil parameter sets predict settlements within the measured range. It is concluded that in reality ground conditions are inhomogeneous and/or the behaviour is influenced by stratification and discontinuities.

Surface settlements obtained from Finite Element analysis are in good agreement with the empirical distribution by Peck (1969) and Attwell and Woodman (1982).

In 2D FE-analysis two different MStage-factors for the pre-relaxation phase and for the installation of the shotcrete lining were used. The load reduction factors were obtained by matching results in 2D and 3D analysis. The load reduction factor MStage = 1 – β used in the 2D pre-relaxation phase is highly influenced by the used reference value:

- For calibration with crown settlements, steady state conditions are predicted with ±5%.
- Matching crown settlements in the middle of the excavation length results in large MStage-values, 0.65 – 0.80 in drained analysis and 0.55 – 0.63 in undrained analysis. It is influenced by the sagging of the tunnel crown in 3D calculations. The predicted surface settlements are overestimated.
- By matching crown settlements at the end of the excavation length the predicted steady state surface settlements and axial forces are in good agreement with the result of 3D analysis. The applied MStage-values range from 0.63 to 0.78 in drained analysis and 0.56 and 0.64 in undrained analysis
- The calibration of the 2D model using surface settlements results in the lowest pre- relaxation factors. Because the influence of lining installation on surface deformations is small, a reliable determination of the second pre-relaxation factor and the prediction of steady state settlements are not possible.
- When matching axial forces in 2D and 3D only one MStage-value can be determined. The determination of the maximum axial force for calibration is difficult due to the uneven distribution of lining forces in PLAXIS 3D 2011. Reliable results are only obtained for calibration with the final axial forces. Predicted crown and surface settlements are in good agreement for drained analysis.

Generally MStage of drained calculations exceed the values of undrained calculations, because volumetric changes are restricted due to incompressible pore water and the applied load reduction factor is related to the magnitude of reference settlements.

The constitutive model influences the load reduction factor. The use of the Mohr-Coulomb model results in lower MStage-values than the Hardening Soil model. MStage obtained from computations considering small strain stiffness (HS-small) is higher than the corresponding values from the standard HS model. The HS-small model is very sensitive to changes of MStage. Different stiffness parameters have little influence on the obtained load-reduction factors unlike an existing pre-overburden pressure. MStage-values obtained from the calculations using the HS model with POP = 500 kN/m² are larger than for the corresponding computations without POP. Stiffer soils result in slightly higher MStage-values.

REFERENCES

[1]. S. Möller, Tunnel induced settlements and structural forces in linings, Bd. Mitteilung 54 des Instituts für Geotechnik, P. Vermeer, Hrsg., Universität Stuttgart, 2006.

[2]. Plaxis bv, PLAXIS 3D 2011 Manual, Delft, The Netherlands, 2011.

[3]. T. Schanz, P. A. Vermeer und P. Bonnier, The hardening soil model: Formulation and verification, Rotterdam, The Netherlands: Balkema, 1999.

[4]. P. W. Rowe, „The stress-dilatiancy relation for static equilibrium of an assembly of particles in contract,"Proceeding of the Royal Society A. 296, pp. 500-527, 9 October 1962.

[5]. T. Benz, Small-Strain Stiffness of Soils and its Numerical Consequences, Bd. Mitteilung 55 des Instituts für Geotechnik, P. Vermeer, Hrsg., Universität Stuttgart, 2007.

[6]. H. F. Schweiger, Computational Geotechnics - Lecture Notes, Graz: Institute for Soil Mechanics and Foundation Engineering, 2011.

[7]. B. Moritz, H. Goldberger und P. Schubert, „Application of the Observational Method in

Heterogeneous Rock Mass with Low Overburden,“ Felsbau 24, Nr. 1, pp. 62-72, 2006.

[8]. H. Meißner, „Tunnelbau unter Tage, Empfehlungen des Arbeitskreis 1.6 "Numerik in der Geotechnik" Abschnitt 2,“ Geotechnik 19, pp. 99-108, 1996.

[9]. GEOCONSULT ZT GmbH, Geotechnische Dokumentation - Tunnelbau, B1260 Erkundungstunnel Mitterpichling, ÖBB Bau AG, 2009.

[10]. GEOCONSULT ZT GmbH, Geomechanische Prognose - B1258 Erkundungstunnel Paierdorf, 2003.

[11]. Plaxis bv, Plaxis 2D 2011 Manual, Delft, The Netherlands, 2011.

[12]. M. Wohlfahrt, Diplomarbeit: Anhang-Erkunndungstunnel Mitterpichling Ost, Graz: Institut für Bodenmechanik und Grundbau, 2010.

[13]. M. Wehnert, Ein Beitrag zur drainierten und undrainierten Analyse in der Geotechnik, Mitteilung 53 des Institut für Geotechnik Hrsg., P. Vermeer, Hrsg., Universität Stuttgart, 2006.

[14]. H. F. Schweiger, „Some remarks on Pore Pressure Parameters A and B in Undrained Analyses with the Hardening Soil Model,“ Plaxis Bulletin 12, pp. 6 - 8, 2002. NUMERICAL MODELLING OF TUNNEL INDUCED SETTLEMENT USING FINITE ELEMENT ANALYSIS SOFTWARE PLAXIS

[15]. R. J. Mair und T. R. N., Theme lecture: Bored tunneling in the urban enviroment, Hamburg: 14th ISSMFE, 1997.

[16]. R. N. Hwang, C. B. Fan und G. R. Yang, „Consolidation settlements due to tunneling,“ Proceedings of South East Asian Symposium on Tunneling and Underground Space Development, pp. 79-86, 18-19 January 1995.

[17]. R. B. Peck, „Deep Excavations and Tunneling in Soft Ground,“ Proceedings of the 7th International Conference on Soil Mechanics and Foundation Engineering, pp. 225- 290,

[18]. P. B. Attewell und J. P. Woodman, „Predicting the dynamics of ground settlements and its derivatives caused by tunneling in soil,“ Ground Engeneering, pp. 13-22, November 1982.

[19]. K. Schikora und T. Fink, „Berechnungsmethoden moderner bergmännischer Bauweisen beim U-Bahn-Bau,“ Bauingenieur 57, pp. 193-198, 1982.

[20]. C. W. W. Ng und G. T. K. Lee, „Three-dimensional ground settlements and stresstransfer mechanisms due to open-face tunnelling,“ Canadian Geotechnical Journal 42, pp. 1015-1029, 2005